



## Mechanism of pyridine bases prepared from acrolein and ammonia by in situ infrared spectroscopy

Xian Zhang<sup>a,b</sup>, Zhen Wu<sup>b,c</sup>, Zi-sheng Chao<sup>d,\*</sup>

<sup>a</sup> Department of Chemical Engineering, School of Erdos, Inner Mongolia University, Erdos 017000, China

<sup>b</sup> Redbud Innovation Institute of Erdos, Erdos 017000, China

<sup>c</sup> Membrane Technology and Engineering Research Center, Department of Chemical Engineering, Tsinghua University, Beijing 100083, China

<sup>d</sup> State Key Laboratory of Chemo/Biosensing and Chemometrics, College of Chemistry and Chemical Engineering, Hunan University, Changsha 410082, China



### ARTICLE INFO

#### Article history:

Received 3 July 2015

Received in revised form 13 August 2015

Accepted 13 August 2015

Available online 18 August 2015

#### Keywords:

Acrolein

Pyridine

3-Picoline

In situ infrared

Mechanism

### ABSTRACT

The in situ infrared spectroscopy of acrolein and ammonia over HF/MgZSM-5 was investigated to check the adsorption reaction of acrolein and ammonia. It was proved that propylene imine intermediate came up during the condensation process of adsorbed acrolein with ammonia. The strong adsorption of C=O helps the formation of propylene imine. The reaction order and active energy were calculated according to the intensity of acrolein infrared spectroscopy. The synthesis of 3-picoline is likely to go through a flat adsorption of propylene imine and a deamination of amino dihydropyridine.

© 2015 Published by Elsevier B.V.

## 1. Introduction

3-Picoline is an important chemical intermediate in the synthesis of pharmaceuticals, agriculture and fine chemicals [1,2]. Pyridine and 3-picoline was prepared from acrolein and ammonia because of a higher yield with no 4-picoline [3], comparing to that from formaldehyde, acetaldehyde and ammonia [4]. The Chichibabin mechanism [5,6] shows that the production of pyridines from saturated aldehyde and ammonia involves imine intermediate. Although, there is still no detailed mechanism for the condensation of acrolein and ammonia to 3-picoline, so that the fact that no 3-picoline could be produced between acetaldehyde and ammonia reaction, where the products are 2-picoline and 4-picoline [7], is paid little attention to and admitted in some literatures [8,9].

Acrolein was considered to be the reaction intermediate in the condensation of formaldehyde, acetaldehyde and ammonia, as pyridine and 3-picoline were the common pyridine products comparing to that of acrolein and ammonia [4]. And also, it was

reported that the production of 3-picoline undergoes a process of propylene imine formation [10], which was confirmed but never investigated until now. Literatures [8,10–12] reported that the formation of 3-picoline from acrolein or propylene imine underwent a hydrogenation and dehydrogenation process, which is inconsistent with the result of 3-picoline prepared from acrolein and ammonium acetate in acetic acid solution with a liquid-phase reactor [13].

Caibin Wang and Li [14] concluded that the catalyst reactive sites in favor of 3-picoline product were Brønsted acid sites over HF-Al<sub>2</sub>O<sub>3</sub> catalyst, however, Ivanova et al. [15] insisted on the interaction of weak Lewis acid sites and Brønsted acid sites of Al<sub>2</sub>O<sub>3</sub>-SiO<sub>2</sub> catalyst. On the other hand, a strong Lewis acid site favored decomposition to pyridine product and polymerization to tars products, while, the Brønsted acid sites were less important than the Lewis ones. Ivanova et al. [16] preferred to the presence of two types of Lewis acid sites exhibiting high activity and selectivity to 3-picoline over SO<sub>4</sub><sup>2-</sup>/TiO<sub>2</sub> catalyst. It is necessary to analyze and study further the catalysis of acid sites for abrogating theses arguments. And also, it is not clear that the adsorption of acrolein and formation of pyridine, involving to the decomposition reaction occurring before or after the 3-picoline formation.

\* Corresponding author.

E-mail addresses: [zschoao@yahoo.com](mailto:zschoao@yahoo.com), [zschoao@hnu.edu.cn](mailto:zschoao@hnu.edu.cn) (Z.-s. Chao).

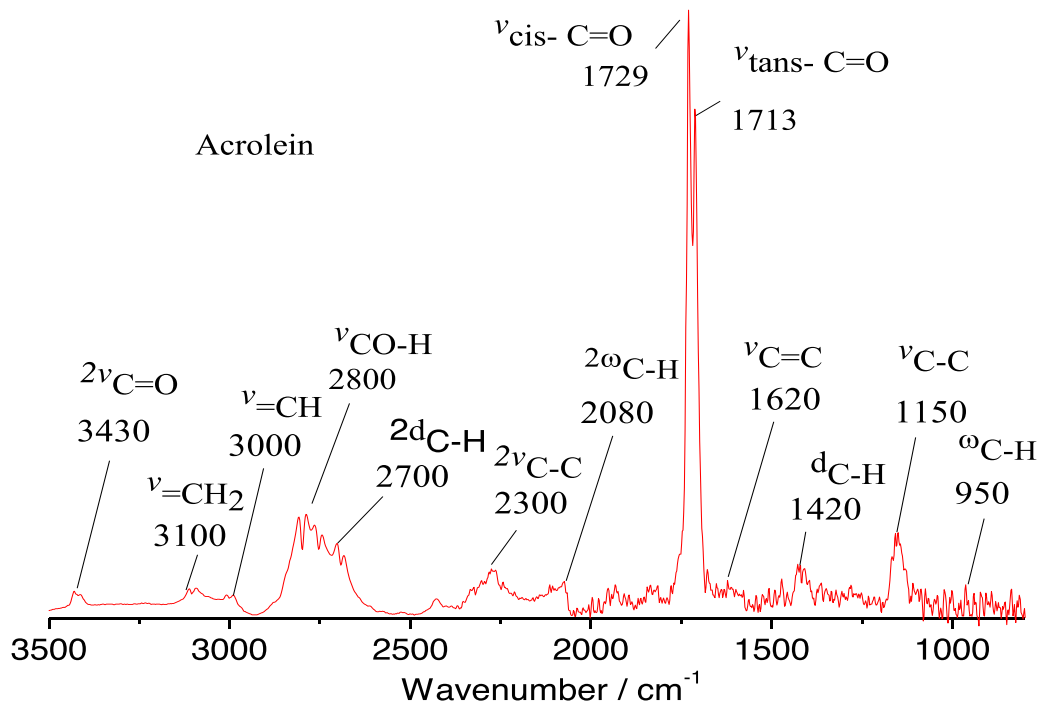


**Fig. 1.** FT-IR spectrum of acrolein at room temperature.

The present study describes the adsorption and reaction of acrolein and ammonia over HF/MgZSM-5 catalyst by in-situ infrared spectroscopy in order to understand the mechanism of pyridine and 3-picoline formation.

## 2. Experimental

### 2.1. Catalyst preparation

The catalyst were modified by impregnation of 130 g of HZSM-5(Si/Al = 25, Nankai University Catalyst Factory) with 100 mL 0.62 M Mg(NO<sub>3</sub>)<sub>2</sub> solution at a temperature 90 °C for 8 h and then dried. After that, 100 mL 0.62 M NH<sub>4</sub>HF<sub>2</sub> solution followed to impregnate the prepared solid with the same condition and then calcinated at 700 °C for 4 h to get a HF/MgZSM-5 catalyst.

### 2.2. Characterization and methods

A varian 3100 FT-IR spectroscopy with a MCT detector and a quartz in-situ IR transmission cell-reactor with a CaF<sub>2</sub> window (Dalian Institute of Chemical Physics, Chinese Academy of Sciences) and a oil diffusion pump vacuum system are used to record the IR spectrums of acrolein and its reaction products. The IR detecting condition was followed as: speed = 40 KHz, filter = 5 Hz, resolution = 2 cm<sup>-1</sup>, under sampling ratio = 2, sensitivity = 1, Co-add = 32, wavenumber = 4000–400 cm<sup>-1</sup>.

### 2.3. Experimental procedure

Acrolein with 95% (in mass), supplied by HuBei Xinjing new material limited company, was firstly purified through distillation before used. Ammonia was supplied by heating commercial ammonium acetate (AR). Potassium bromide was appropriate for IR spectroscopy and supplied by Germany Meck Company.

The procedure was conducted as following: (1) The HF/MgZSM-5 catalyst and KBr were firstly mixed and milled with a mass ration of 1:99 at a total weight of 175 mg, and then pressed into a self-supported 13 mm transparent wafer. The wafer was mounted

**Table 1**  
Wavenumber and assignments of IR spectra of acrolein.

Wavenumber cm <sup>-1</sup>	Bond	Assignments	Intensity
3468–3395	C=O	2ν	Weak
3200–3050	=CH <sub>2</sub>	ν	Weak
3050–2950	=CH—	ν	Weak
2950–2750	CO—H	ν	Strong
2750–2600	C—H	2δ	Medium
2380–2200	C—C	2ν	Medium
2200–2040	C—H	2g	Medium
1750–1660	HC=O	ν	Strong
1630–1550	C=C	ν	Weak
1438–1250	C—H	δ	Medium
1180–1109	C—C	d	Medium
1000–800	C—H	g	Weak

Note: ν, δ and g denote stretching, bending and deformation; 2 denotes the double frequency.

into the sample holder of the IR cell-reactor and then removed the impurities at 350 °C for 2 h under vacuum condition. After the temperature was cooled down, the background spectrum was collected. (2) Then, acrolein was inhaled and adsorbed on the catalyst wafer, at the same time, the adsorption and desorption IR spectrum of acrolein were recorded at various temperature and vacuity. (3) The in situ IR spectrums of adsorbed acrolein were recorded after fresh acrolein and ammonia was inhaled respectively. (4) After ammonia and acrolein was inhaled orderly, the in situ IR spectrums of ammonia condensation with acrolein were recorded at various temperature and time.

## 3. Results and discussion

### 3.1. IR spectrum of acrolein

On the basis of the vibrational spectroscopic study of acrolein as reported [17], we made tentative assignments to IR bands in Fig. 1,

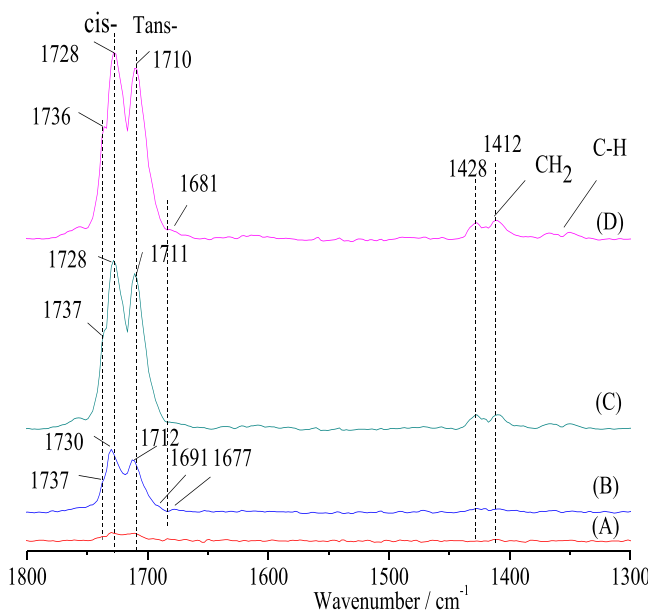
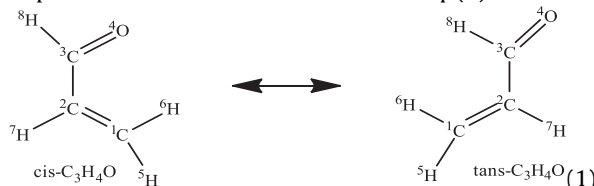


**Fig. 2.** FT-IR spectrum of acrolein at different vacuums: (A) 10 Pa; (B) 50 Pa; (C) 100 Pa; (D) 200 Pa.

which are listed in **Table 1**. The vibration peaks are in pair because of the presence of *cis*- and *trans*- acrolein as Eq. (1).



The spectrum gives rise to C=O stretching bands at 1729 and 1713 cm<sup>-1</sup>, which are assigned to *cis* and *trans* conformations [18], respectively. More *cis*-acrolein, who is more stable than *trans*-one, has been observed as its intensity is stronger.

The vibration intensities of acrolein depress greatly at lower vacuum, so that only the C=O stretching vibration ( $\nu_{\text{C=O}}$ ) could be observed at 10 Pa as seen in **Fig. 2**. At the same time, the  $\nu_{\text{C=O}}$  frequencies of *cis*- and *trans*-acrolein (1728 and 1710 cm<sup>-1</sup>) are observed at a higher frequency (1730 and 1712 cm<sup>-1</sup>), with new bands at 1691 and 1677 cm<sup>-1</sup>, which are shifted to higher and lower frequency from 1681 cm<sup>-1</sup> respectively, are assigned to weaker and stronger C=O top adsorption of *trans*-acrolein, comparing the band at 1737 cm<sup>-1</sup> is assigned to weak C=C adsorption of *cis*-acrolein [19]. Presumably, we apply these results to a weakened conjugation effect and a strengthened physical adsorption at lower vacuum, as a result that the physical adsorption of C=O leads to a red shift, while that of C=C leads to a blue one [20].

Expect for the same bands shown in Figs. 2 A and 3 A and B at lower temperature, **Fig. 3C** and D exhibit new IR bands due to adsorbed acrolein. The new bands at 1720–1660 cm<sup>-1</sup> in **Fig. 3C** and D are assigned to  $\nu_{\text{C=O}}$  of adsorbed *trans*-acrolein, which is due to the further adsorption and weaker conjugation at higher temperature. While, the bands at 1715 and 1701 cm<sup>-1</sup> in **Fig. 3D** are assigned to blue shift from 1712 cm<sup>-1</sup> and red shift from 1705 cm<sup>-1</sup> of *trans*-acrolein  $\nu_{\text{C=O}}$  respectively. The 1701 cm<sup>-1</sup> is probable due to flat adsorption of *cis*-acrolein, but the band at 1726 and 1698 cm<sup>-1</sup>, red-shifted respectively from 1730 and 1701 cm<sup>-1</sup> at the same time, are also considered to be the further C=O adsorption after C=C adsorbed [21,22]. New weak signals for  $\nu_{\text{C=O}}$  bands at 1691–1660 cm<sup>-1</sup> in **Fig. 3D** suggest stronger adsorption of *trans*-acrolein or acrolein dimmers for the dimerization of acrolein at

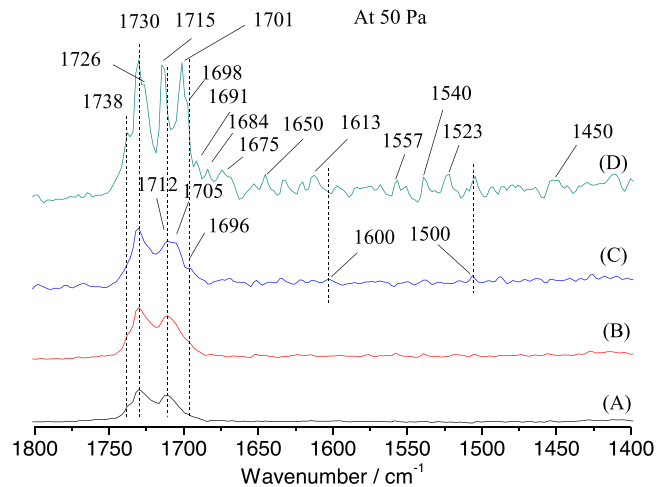


**Fig. 3.** FT-IR spectrum of acrolein at different temperature: (A) 100 °C; (B) 175 °C; (C) 250 °C; (D) 325 °C. (For interpretation of the references to color in this text, the reader is referred to the web version of this article.)

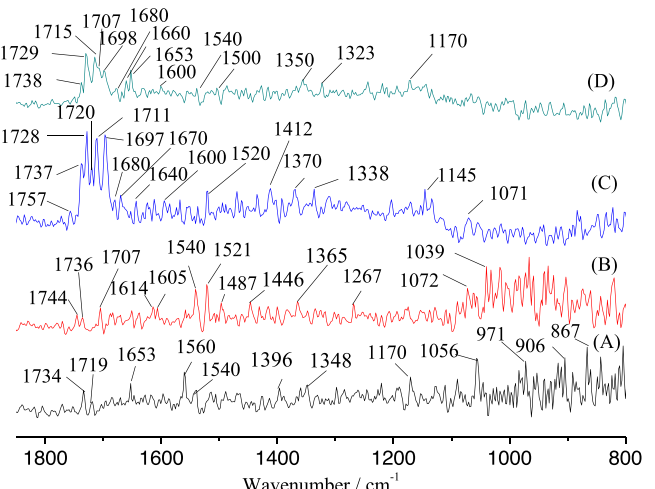


**Fig. 4.** FT-IR spectrum of adsorbed acrolein at 325 °C when fresh acrolein was inhaled: (A) at 30 Pa before; (B) at 10 Pa before; (C) after for 30 s; (D) after for 60 s.

higher temperature may produce various ketene, olefin and conjugated 2-methyl-2,4-pentadinalen (1680–1450 cm<sup>-1</sup>) [23].

**Fig. 4** displays IR spectra of acrolein at 325 °C before and after fresh acrolein was inhaled. Bands of *trans*-acrolein  $\nu_{\text{C=O}}$  disappear to form multi-conjugated aldehyde (1653 cm<sup>-1</sup>), conjugated alkenes (1560 and 1540 cm<sup>-1</sup>) and ether species (1056 cm<sup>-1</sup>) because of the C=O strong adsorption as seen in **Fig. 4A** [24]. Additional peak at 1719 cm<sup>-1</sup> is assigned to C=O adsorbed of *cis*-acrolein, which adsorbed more strongly appear in **Fig. 4B** at lower pressure, while 1744 cm<sup>-1</sup> is due to  $\nu_{\text{C=O}}$  from adsorbed aliphatic aldehyde and 1707 cm<sup>-1</sup> from the *trans*-one, comparing to 1170 cm<sup>-1</sup> from  $\nu_{\text{C-C}}$  of adsorbed acrolein [25,26]. Further more, peaks of  $\nu_{\text{C-C}}$  shift to 1614 and 1605 cm<sup>-1</sup>, conjugated  $\nu_{\text{C=C}}$  shift to 1540 and 1521 cm<sup>-1</sup>,  $\nu_{\text{C-C}}$  shift to 1365 and 1267 cm<sup>-1</sup> and  $\nu_{\text{C-O}}$  shift to 1072 and 1039 cm<sup>-1</sup> because of stronger adsorption. After fresh acrolein is dosed, the adsorption of acrolein becomes weaker that freedom phase (1728 and 1711 cm<sup>-1</sup>), aliphatic aldehyde (1757 cm<sup>-1</sup>) and adsorbed phase (1737, 1720, 1697, 1680 and 1670 cm<sup>-1</sup>) are observed in **Fig. 3C**. The vibrations at 1660–1000 cm<sup>-1</sup> become more, but only olefin (1600, 1520 cm<sup>-1</sup>),  $\nu_{\text{C-H}}$  (1412, 1370 and 1338 cm<sup>-1</sup>),  $\nu_{\text{C-C}}$  (1145 cm<sup>-1</sup>) and  $\nu_{\text{C-O}}$  (1071 cm<sup>-1</sup>) are obvious. For a long time, the intensity of adsorbed acrolein, especially the band at 1698 cm<sup>-1</sup>, becomes weaker and the bands of

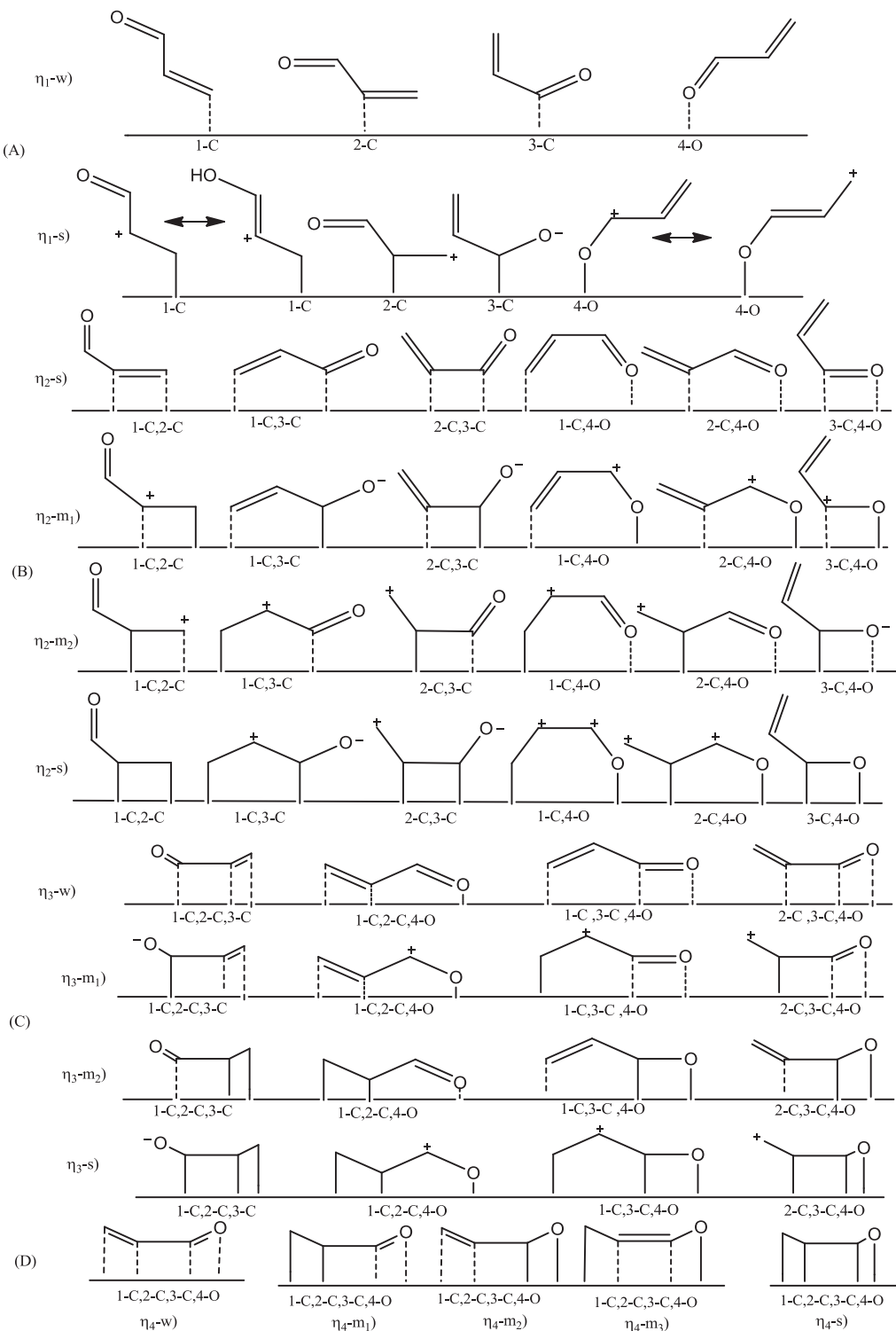


**Fig. 5.** Adsorption forms of acrolein over catalyst surface.

non-conjugated aldehyde ( $1757\text{ cm}^{-1}$ ) and flat-adsorbed phase ( $1720\text{ cm}^{-1}$ ) disappear in Fig. 4D. It is suggested that the reaction of acrolein caused by flat-adsorbed and point-adsorbed acrolein as new bands of multi-conjugated  $\nu_{\text{C=O}}$  ( $1660$  and  $1653\text{ cm}^{-1}$ ) could be seen, at the same time, other bands of  $\nu_{\text{C=C}}$  decrease as their weaker adsorption with the catalyst.

Above all, it is said that *trans*-crolein is more active and easier to be adsorbed than *cis*-crolein, of which  $\text{C}=\text{C}$  is easier to be adsorbed than  $\text{C}=\text{O}$  comparing that of *trans*-crolein is opposite.

The adsorption of acrolein will draw stronger and flatter at higher temperature and lower pressure, when acrolein will polymerize to form dimmers. It is meaning that the weak (w) physical adsorption is converted to medium (m) and strong (s) chemical adsorption and the point adsorption to the flat adsorption. The adsorption will become more complicated as acrolein and its adsorption products would be adsorbed on Brønsted, weaker and stronger Lewis acid sites over the zeolite catalyst surface.

### 3.2. Adsorption of acrolein

The electron affinity of acrolein double bands, which are easy to be adsorbed over catalyst surface as their higher electron density, follow the order:  ${}^1\text{C}=\text{C} > {}^3\text{C}=\text{O} > {}^1\text{C}=\text{C} > {}^3\text{C}=\text{C}$ . The electron density and electrophilic ability of atoms follow the order:  $\text{O} > \text{C} \approx {}^1\text{C} > {}^3\text{C}$ , so that a single point adsorption ( $\eta_1-\sigma$ ) of the oxygen atom happens more easily on  ${}^3\text{C}=\text{O}$ , while a dual site adsorption ( $\eta_2-\pi$ ) of  ${}^1\text{C}=\text{C}$  is priority. The adsorption of acrolein, which is determined to the surface structure [27,28], environment [29] and properties [30,31], is followed in Fig. 5 as summarized by the count of adsorption sites.

(A) The single point ( $\eta_1$ ) adsorption. The  $\eta_1-\text{s}$  adsorption of signal atom will produce a carbenium ion, which is not steady and difficult to be observed as seen in Fig. 5A-s. Only the  $[{}^4\text{O}]$   $\eta_1-\text{w}$  adsorption of *trans*-acrolein shown in Fig. 5A-w could be observed clearly as it is full of unpaired electron. Comparatively, the  $\eta_1-\text{w}$  adsorption of other atoms is so weak that their vibration is consistent with that of unabsorbed acrolein.

(B) The double points ( $\eta_2$ ) adsorption. Due to the lowest electron density, the  $\eta_2-\text{w}$  adsorption of acrolein containing 3-C could be observed difficultly except for that of  $[{}^3\text{C}, {}^4\text{O}]$ , comparing that containing 4-O will make the  $\nu_{\text{C}=\text{O}}$  red shift. On the contrary, the  $\eta_2-\text{w}$  adsorption of  $[{}^1\text{C}, {}^2\text{C}]$  will make a blue shift. Because of the conformation resistance, the  $\eta_2-\text{w}$  adsorption is more possibly happened to the *cis*-acrolein than *trans*-acrolein. The  $\eta_2-\text{m}$  and  $\eta_2-\text{s}$  adsorption of acrolein except for that of  $[{}^1\text{C}, {}^2\text{C}]$ , producing aliphatic aldehyde, and  $[{}^3\text{C}, {}^4\text{O}]$ , producing ether, could not be observed because of their activation as seen in Fig. 5B.

(C) The three points ( $\eta_3$ ) adsorption. As the same reason above, the  $\eta_3-\text{s}$  and  $\eta_3-\text{m}_1$  adsorption of acrolein could not be observed because of the carbonion formation. Due to the atom electron density order of acrolein, the  $\eta_3-\text{w}$  and  $\eta_3-\text{m}_2$  adsorption of  $[{}^1\text{C}, {}^2\text{C}, {}^4\text{O}]$ , which are due to the further  $\eta_2-\text{w}$  and  $\eta_2-\text{s}$  adsorption of  $[{}^1\text{C}, {}^2\text{C}]$  respectively, is the more possible one than the others as seen in Fig. 5C-w and C-m<sub>2</sub>.

(D) The four points ( $\eta_4$ ) adsorption. The  $\eta_4$  adsorption of acrolein, which is usually called flat adsorption as all atoms interact with the surface as seen in Fig. 5D, is attributed to the  $\eta_3$  further adsorption that the  $\eta_4-\text{m}_2$  and  $\eta_4-\text{m}_3$  adsorption of acrolein could hardly be observed. Due to the coadsorption of both  $\text{C}=\text{C}$  and  $\text{C}=\text{O}$ , the energy and stability of  $\eta_4-\text{w}$  adsorption increase and are close to that of  $\eta_2-\text{s}$  adsorption. The  $\eta_4-\text{m}_1$  and  $\eta_4-\text{s}$  adsorption need so more energies that the acrolein may probably decompose at some extent.

The  $\pi$ , di- $\sigma$  and di- $\pi$  adsorption reported in literatures [32,33] are correspond to  $\eta_2-\text{w}$ ,  $\eta_2-\text{s}$ , and  $\eta_4-\text{w}$  adsorption. Except for the weak physisorption, Loffreda [17] reported the strong adsorption of  $[{}^4\text{O}]$  *trans*- $\eta_1$ ,  $[{}^1\text{C}, {}^2\text{C}]$  *trans*- and *cis*- $\eta_2$ ,  $[{}^3\text{C}, {}^4\text{O}]$  *trans*- $\eta_2$ ,  $[{}^1\text{C}, {}^2\text{C}, {}^4\text{O}]$  *trans*- and *cis*- $\eta_3$ , *trans*- and *cis*- $\eta_4$  were present over Lewis acid sites. Akita [29] admitted that as the coverage increasing, *cis*- $\eta_3$  and *trans*- $\eta_4$  adsorption, which is more stable than *trans*- $\eta_1$  adsorption, will be converted to *trans*- and *cis*- $\eta_2-\text{s}$  adsorption. After all, it is difficult to confirm the active carbonion intermediate from strong adsorption. Although, we could conclude that flat, strong and *trans* adsorption are favored at lower pressure, while point, strong and *cis* adsorption are favored at higher temperature and stronger acid sites and adsorption of  $\text{C}=\text{O}$  is favored over polar surface, on the contrary, that of  $\text{C}=\text{C}$  is favored over non-polar surface.

Based on the vibrational spectroscopic studies of acrolein under various condition, we made tentative assignments to IR bands are listed in Table 2. Therefore, the  $\eta_1-\text{w}$  and  $\eta_2-\text{w}$  adsorption of and gaseous acrolein are present at low pressure as seen in Fig. 2B. The  $\eta_2-\text{s}$ , *trans*- $\eta_3-\text{w}$  and *trans*- $\eta_4-\text{w}$  adsorption of acrolein are present at high temperature as seen in Fig. 3D, comparing the  $\eta_3-\text{m}$ , *cis*-

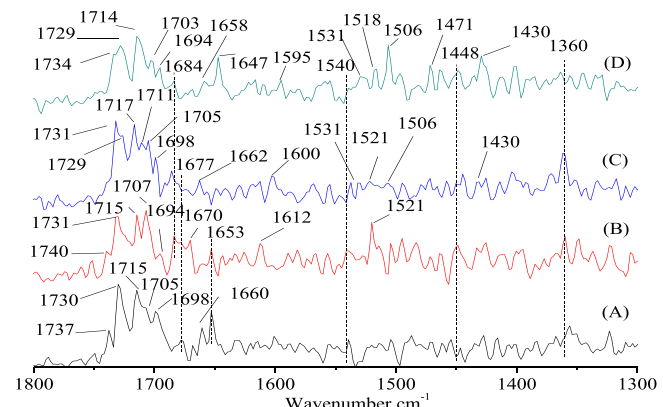


**Fig. 6.** FT-IR spectrum of acrolein and ammonia: (A) before  $\text{NH}_3$  inhaled; (B) after  $\text{NH}_3$  inhaled for 1 min; (C) after  $\text{NH}_3$  inhaled for 18 min. (For interpretation of the references to color in the text, the reader is referred to the web version of this article.)

$\eta_3-\text{w}$  and *cis*- $\eta_4-\text{w}$  and adsorption at high temperature and low pressure in Fig. 4A, meanwhile, the  $\eta_3-\text{m}$ ,  $\eta_3-\text{m}$  and  $\eta_4-\text{s}$  at high temperature and lower pressure in Fig. 4B.

### 3.3. Reaction of acrolein and ammonia

Fig. 6 shows the adsorption spectra of acrolein before and after  $\text{NH}_3$  inhaled for a time. After  $\text{NH}_3$  was dosed for 1 min comparing Fig. 6B to Fig. 6A, one can see that *cis*-, *trans*- $\eta_2-\text{w}$   $[{}^1\text{C}, {}^2\text{C}]$  and *trans*- $\eta_1-\text{w}$  adsorption of acrolein decrease while *trans*- $\eta_3-\text{w}$  adsorption of acrolein keeps unchanged. At the same time, the new band at  $1670\text{ cm}^{-1}$  observed in Fig. 6B appear indicating the existence of  $\text{C}=\text{N}$  group [34], with also a *trans*- $\eta_2-\text{w}$   $[{}^3\text{C}, {}^4\text{O}]$  adsorbed  $\text{C}=\text{O}$  band at  $1684\text{ cm}^{-1}$  blue shifted from  $1677\text{ cm}^{-1}$ . It says that the acrolein have been converted to propylene imine, who is probably a *cis*-one as the  $\eta_1-\text{w}$  adsorption of *trans*- acrolein is depressed most greatly. That the *trans*- $\eta_1-\text{w}$  band at  $1698\text{ cm}^{-1}$  shifts to  $1694\text{ cm}^{-1}$  shows also a weaker adsorption after  $\text{NH}_3$  dosed in Fig 6B and D. The bands at  $1660$  and  $1653\text{ cm}^{-1}$  disappear gradually and a new band at  $1647\text{ cm}^{-1}$  is easy to be considered to be a multi-conjugated  $\nu_{\text{C}=\text{N}}$ . Additionally, the new bands at  $1612$  and  $1521\text{ cm}^{-1}$  indicate the conjugated  $\text{C}=\text{C}$  or cyclic  $\text{C}=\text{C}$  [23], who was partly converted to olefin [26] at  $1600$  and  $1506\text{ cm}^{-1}$  as seen in Fig 6C and D. And also the  $1360\text{ cm}^{-1}$  band of  $\delta_{\text{C}-\text{H}}$  is shifted to higher frequency as acrolein decrease. Moreover, the new bands at  $1540$  and  $1448\text{ cm}^{-1}$  indicate the existence of pyridine [35], however, more 3-picoline appear at  $1531$  and  $1430\text{ cm}^{-1}$  after a long time [36,37]. It suggests that 3-picoline appears after the production of pyridine, which may be produced at stronger acid sites. As a following,  $\text{NH}_3$  would occupy those strong acid sites leading to weak acid ones and preferring to produce 3-picoline product.

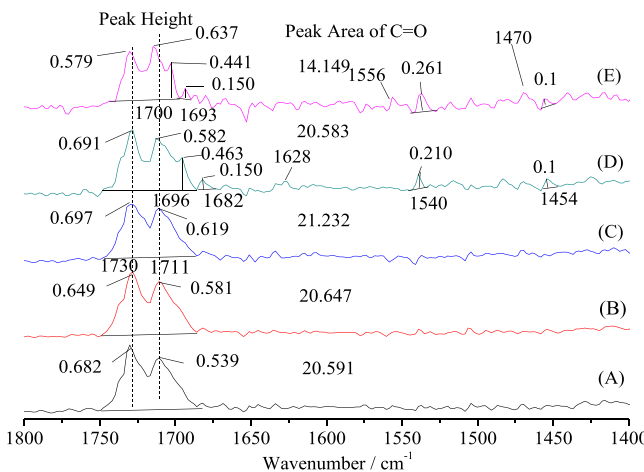
Fig. 7 shows the spectra of acrolein with  $\text{NH}_3$  dosed before acrolein for a certain time at different temperatures. New  $\nu_{\text{C}=\text{O}}$  Bands of adsorbed acrolein at  $1750$ – $1680\text{ cm}^{-1}$  and pyridines at  $1540$  and  $1454\text{ cm}^{-1}$  are observed in Fig. 7D and E. It indicates that pyridines are more easily to be produced when  $\text{NH}_3$  is overdosed before acrolein and at a temperature exceeding  $523\text{ K}$ , at which acrolein is activated by adsorption of *trans*-acrolein. It shows that pyridines are mainly produced from *trans*-acrolein and higher temperature as the intensity of *trans*-acrolein decrease and that of pyridines increase at  $598\text{ K}$  comparing that at  $523\text{ K}$ . However, other bands at  $1556$  and  $1470\text{ cm}^{-1}$  show not only the present of pyridine products but other byproduct.

Fig. 8 shows the  $\text{HC}=\text{O}$  peak area ( $A$ ) of acrolein versus temperature ( $T$ ) and time ( $t$ ), and also the curve of  $\ln(-dA/dt)$  versus  $\ln A$ . The absorbance of acrolein  $\text{HC}=\text{O}$  peak area ( $1750$ – $1680\text{ cm}^{-1}$ ) and its concentration accords with the Lambert-Beer's Law

**Table 2**

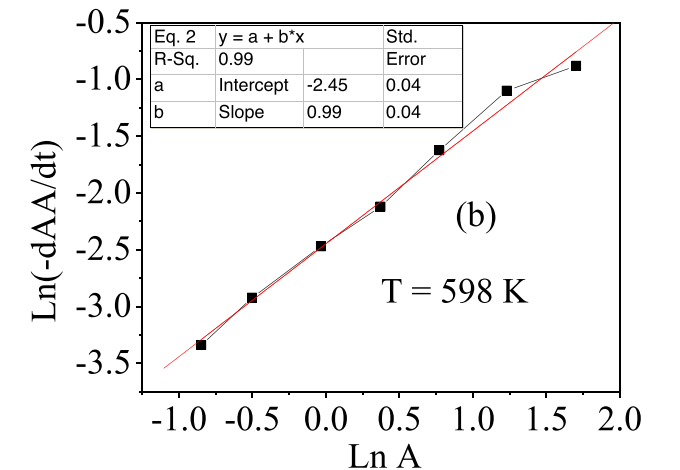
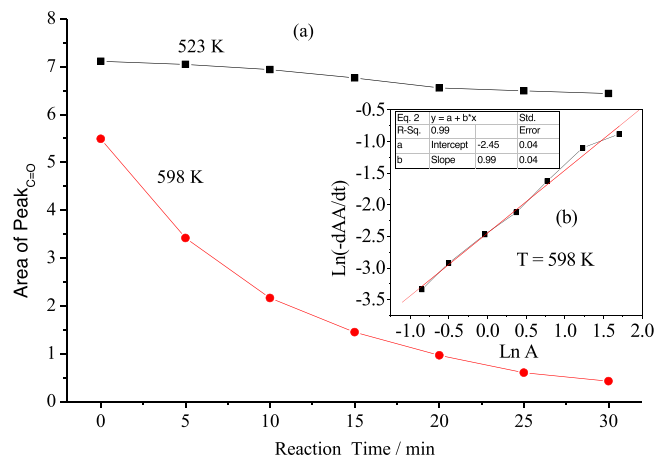
Frequencies and assignments of IR spectra of acrolein adsorption over catalyst surface.

Absorption		HC=O Conjugated	Wavenumber (cm <sup>-1</sup> )	
Types	Atoms		Cis—C <sub>3</sub> H <sub>4</sub> O	Trans—C <sub>3</sub> H <sub>4</sub> O
Gas η <sub>1</sub>	w	None <sup>4</sup> O	Yes Yes	1729–1731 1728
	s	<sup>4</sup> O	No	1145
				1696–1690 1071
η <sub>2</sub>	w	<sup>1</sup> C, <sup>2</sup> C	Yes	1737–1738
	w	<sup>1</sup> C, <sup>4</sup> O; <sup>2</sup> C, <sup>4</sup> O	Yes	1719–1720
	w	<sup>3</sup> C, <sup>4</sup> O	Yes	1726
	s	<sup>1</sup> C, <sup>2</sup> C	No	1684–1675 1757
	s	<sup>3</sup> C, <sup>4</sup> O	No	1172–1056
η <sub>3</sub>	w	<sup>1</sup> C, <sup>2</sup> C, <sup>4</sup> O	Yes	1726
	w	<sup>2</sup> C, <sup>3</sup> C, <sup>4</sup> O	Yes	1719–1720
	w	<sup>1</sup> C, <sup>3</sup> C, <sup>4</sup> O	Yes	1719–1720
	m <sub>2</sub>	<sup>1</sup> C, <sup>2</sup> C, <sup>4</sup> O	No	1744
η <sub>4</sub>	w	<sup>1</sup> C, <sup>2</sup> C, <sup>3</sup> C, <sup>4</sup> O	Yes	1726
	m <sub>1</sub>	<sup>1</sup> C, <sup>2</sup> C, <sup>3</sup> C, <sup>4</sup> O	No	1736
	s	C, <sup>2</sup> C, <sup>3</sup> C, <sup>4</sup> O	No	1072–1039

**Fig. 7.** FT-IR spectra of ammonia and acrolein for 30 min at different temperatures: (A) 298 K; (B) 373 K; (C) 448 K; (D) 523 K; (E) 598 K.

[38]:  $A = K \times C$  (the value of molar absorptivity  $K$  is a constant,  $L \times mol^{-1} \times cm^{-1}$ ). The conversion ( $\alpha$ ) of HC=O group, which is consistent with that of acrolein at this low pressure, is calculated as  $\alpha = (A_0 - A_t)/A_0 \times 100\% = 92.21\%$  when  $T = 598$  K and  $t = 30$  min in Fig. 8a. For that, the initial HC=O absorbance of acrolein is described for  $A_0$ , and the absorbance of acrolein at  $t$  moment is described for  $A_t$ . The equation of reaction rate for acrolein and ammonia is evolved as Eq. (2), in which  $k$  is the reaction velocity constant ( $k, min^{-1}$ ) and  $n$  is the reaction order ( $n$ ). The reaction order  $n$  is consistent with the curve slope of  $\ln(-dA/dt)$  versus  $\ln A$  in Fig. 8b. The results show the standard curve function:  $y = a + b \times x = -2.4477 + 0.9932 \times x$ , and the square of linear correlation coefficient:  $R^2 = 0.9906$ . It shows  $n = 0.9932 \approx 1$ , which meaning the  $\ln(-dA/dt)$ – $\ln A$  curve is consisted with the first-order kinetics mode. Probably, propylene imine is the first main intermediate from acrolein and ammonia and HC=O group is the main activated site [11,12].

$$\begin{aligned} v &= \frac{-dC}{dt} = k \times C^n \Rightarrow -\frac{1}{K} \times \frac{dA}{dt} = \frac{k}{K^n} \times A^n \Rightarrow -\frac{dA}{dt} = k \times K^{1-n} \times A^n \\ &\Rightarrow \ln(-\frac{dA}{dt}) = \ln(k \times K^{1-n}) + n \times \ln A \end{aligned} \quad (2)$$

**Fig. 8.** Peak area of acrolein HC=O group: (a) versus temperature ( $T$ ) and time ( $t$ ); (b)  $\ln(-dA/dt)$  versus  $\ln A$ . (b) Peak area of acrolein HC=O group  $\ln(-dA/dt)$  versus  $\ln A$ .

As the reaction order  $n$  is equal or approximate to 1, the equation of reaction rate could be evolved as Eq. (3).

$$\begin{aligned} v &= \frac{-dC}{dt} = k \times C \Rightarrow \frac{-dC}{C} = k \times dt \Rightarrow \ln C = \ln C_0 - k \times t \\ &\Rightarrow \ln A = \ln A_0 - k \times t \end{aligned} \quad (3)$$

**Fig. 9** shows the curves of  $\ln A$  versus  $t$  and the curve of  $\ln k$  versus  $1/T$ . The curve slope of  $\ln A$  versus  $t$  shown in **Fig. 9a** is the negative value of the reaction velocity constant ( $k$ ), which is 0.0037 at 523 K and 0.085 at 598 K. The Arrhenius relation could be evolved as Eq. (4), in which  $A^0$  is the Aleniwus factor ( $M^{1/2} \times \text{min}^{-1}$ ) and  $E_a$  is the activity energy.

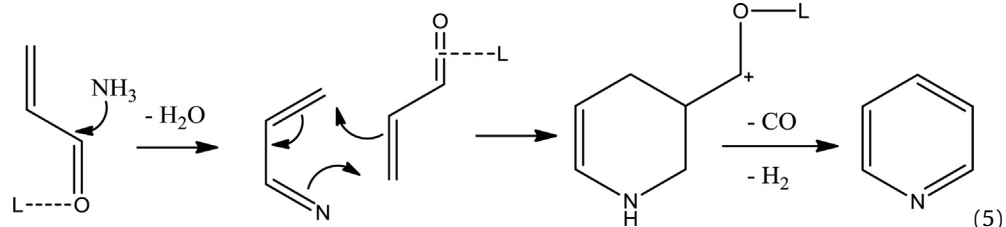
$$k = A^0 \times e^{(-E_a/RT)} \Rightarrow \ln k = \ln A^0 - \frac{E_a}{RT} \quad (4)$$

The curve slope of  $\ln k$  versus  $1/T$  shown in **Fig. 9b** is calculated as  $-E_a/RT = -13163$ , so the activity energy

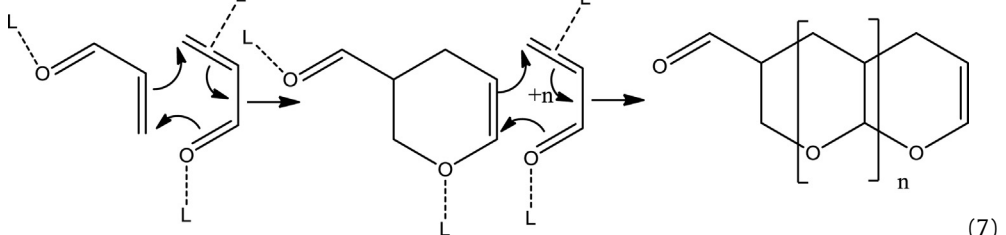
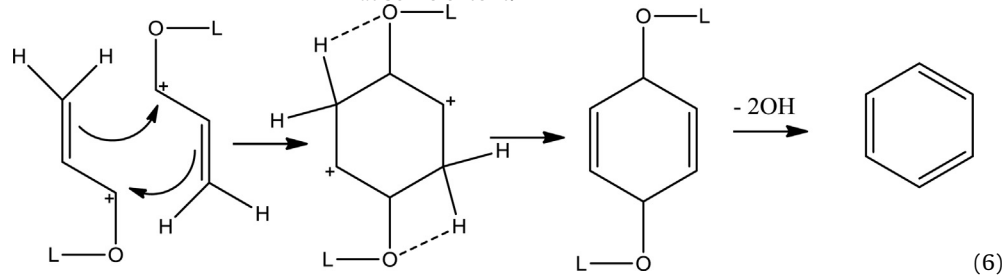
$119 - 16 = 103 \text{ kJ} \times \text{mol}^{-1}$  in *trans*-one with Extended Hückel Mode and ChemBio 3D soft. It is also confirmed that propylene imine is the reaction intermediate as the reaction  $E_a$  is close to the  $\Delta E$  of propylene imine and acrolein.

### 3.4. Mechanism of condensation between acrolein and ammonia

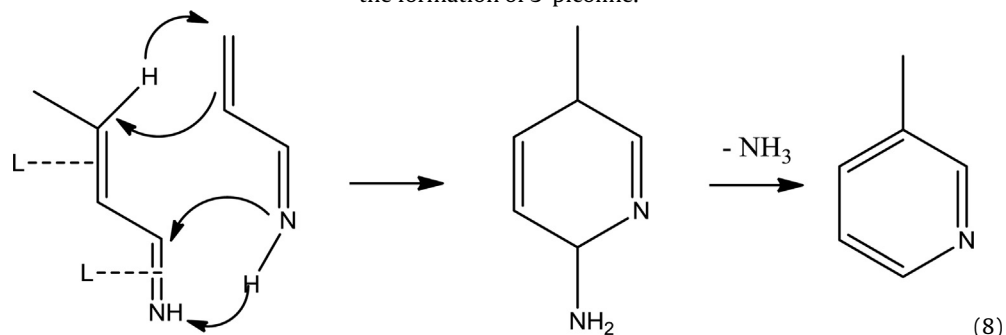
The result that pyridine products is more easily to be produced over stronger Lewis sites is also observed in this paper due to a stronger adsorption of *trans*-acrolein [16]. A Diels–Alder condensation is proposed to be present as shown in Eq. (5), which is similar to the acrolein dimerization and decarbonylation [25].



The stronger C=O adsorption of *trans*-acrolein could also produce olefin products and polymerization products [11,15] as seen in Eqs. (6) and (7), which are related to stronger and *cis*-adsorption at some extent.



The production of 3-picoline is considered to be related to a weak and flat adsorption of *trans*-propylene imine as seen in Eq. (8). As the adsorption over Brønsted and weaker Lewis acid sites are weaker than that over stronger Lewis acid site, the 3-picoline is probably produced on the former two catalytic sites [14,16]. It is concluded that the hydrogenation of acrolein is not necessary for the formation of 3-picoline.



$E_a = 13,163 \times 8.314 = 109.4 \text{ kJ} \times \text{mol}^{-1}$ . The energy difference ( $\Delta E$ ) of propylene imine and acrolein is calculated to be  $120 - 9 = 110 \text{ kJ} \times \text{mol}^{-1}$  in *cis*-conformation and

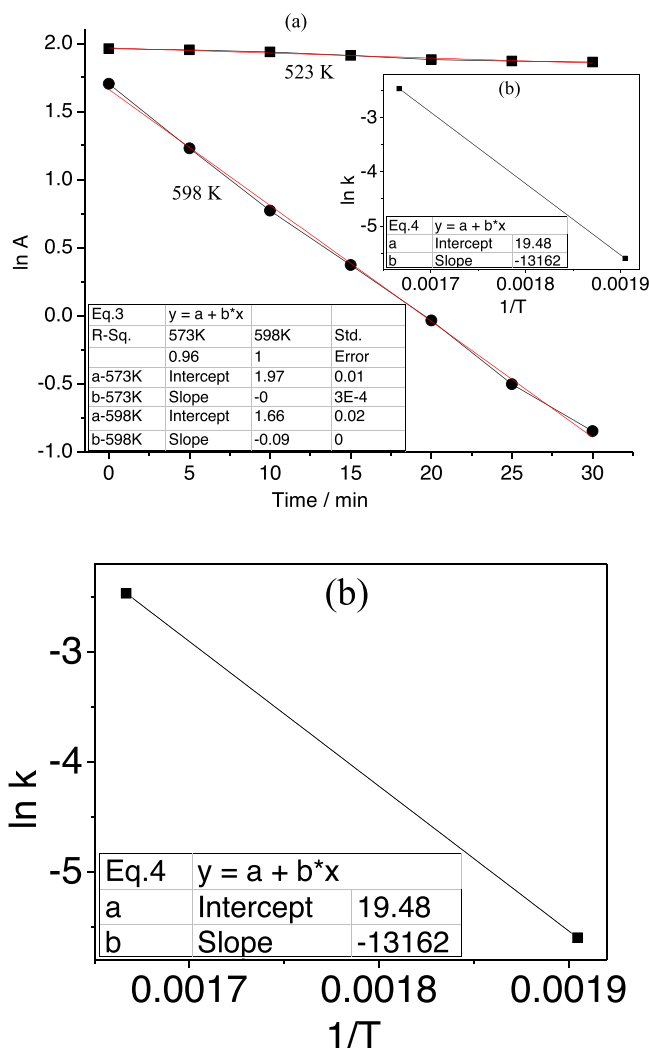


Fig. 9. Peak area of acrolein HC=O group: (a)  $\ln A$  versus  $t$ ; (b)  $\ln k$  versus  $1/T$ . (b) Peak area of acrolein HC=O group  $\ln k$  versus  $1/T$ .

#### 4. Conclusions

Acrolein is activated at 250 °C because of the presence of HC=O and/or C=C weaker adsorption of *trans*-acrolein. The stronger and flat adsorption of *trans*- and *cis*-acrolein at higher temperature and lower pressure would draw acrolein polymerization and decomposition to the formation of multi-conjugated alkene, aldehyde and olefin.

Propylene imine, which is more easily to be produced from adsorbed *trans*-acrolein when ammonia is overdosed, is considered to be the intermediate for the formation of pyridine products during the condensation of acrolein and ammonia. The reaction of acrolein and ammonia is a first order reaction with the activity energy of 109.4 kJ × mol<sup>-1</sup>, which is an approximate value with the energy of acrolein converted to propylene imine.

The pyridine product is produced from *cis*-propylene imine and C=O double-adsorbed *trans*-acrolein through a Diels–Alder reaction and decarbonylation of C=O adsorption over strong Lewis acid site. However, the 3-picoline is preferred to be produced from flat adsorbed *trans*-acrolein and *trans*-propylene imine over Brønsted and weaker Lewis acid sites.

#### Acknowledgements

We are grateful to the financial supports from the Project #21376068 for National Natural Science Foundation (NSFC), the Colleges and Universities' Scientific Research Project of Inner Mongolia Autonomous Region (NJZZ13017) and the Innovation training program of Inner Mongolia University.

#### References

- [1] Y.C. Wei, Fine Spectrosc. Chem. (China) 14 (2006) 1.
- [2] C.L. Liu, C.M. Wang, C.R. Yu, Y.H. She, Pesticide (China) 38 (1999) 1.
- [3] X. Zhang, Z.S. Chao, D.G. Huang, C.W. Luo, W. Liu, K.M. Wang, J.G. Pan, Chem. Ind. Eng. Process. (China) 31 (2012) 1113.
- [4] F. Jin, Y.G. Cui, Z.B. Rui, Y.D. Li, J. Mater. Res. 25 (2010) 271.
- [5] S.K. Roy, B. Ghosh, S.K. Roy, Stud. Surf. Sci. Catal. 113 (1998) 713.
- [6] B. Singh, S.K. Roy, K.P. Sharma, T.K. Goswami, J. Chem. Technol. Biotechnol. 71 (1998) 246.
- [7] M.I. Farberov, V.V. Antonova, B.F. Ustavshchikov, N.A. Titova, Chem. Heterocycl. Compd. 11 (1975) 1349.
- [8] R.S. Sagitullin, G.P. Shkil, I.I. Nosonova, A.A. Ferber, Chem. Heterocycl. Compd. 32 (1996) 127.
- [9] J.J. Li, Chichibabin pyridine synthesis-name reactions in heterocyclic chemistry, John Wiley & Sons Inc., Canada, 2009, pp. 107.
- [10] J.R. Calvin, R.D. Davis, C.H. McAtee, Appl. Catal. A 285 (2005) 1.
- [11] C.B. Wang, Y.R. Li, Chin. J. Pharm. (China) 6 (1984) 1.
- [12] F. Jin, Y.D. Li, Catal. Lett. 131 (2009) 545.
- [13] A. Nicolson, GB Patent 1 240 928 (1971).
- [14] C.B. Wang, Y.R. Li, Chin. J. Catal. (China) 3 (1982) 187.
- [15] G.A. Zenkovets, A.M. Volodin, A.F. Bedilo, E.B. Burgina, E.M. Alkaeva, Kinet. Catal. 38 (1997) 669.
- [16] A.S. Ivanova, E.M. Al'kaeva, V.M. Mastikhin, E.A. Paukshtis, G.N. Kryukova, Kinet. Catal. 37 (1996) 425.
- [17] D. Loffreda, Y. Juguet, F. Delbecq, J.C. Bertolini, P. Sautet, J. Phys. Chem. 108 (2004) 9085.
- [18] S. Fujii, Y. Misono, K. Itoh, Surf. Sci. 277 (1992) 220.
- [19] J.C.D. Jesús, F. Zaera, J. Mol. Catal. 138 (1999) 237.
- [20] A. Yee, S.J. Morrison, H. Idriss, J. Catal. 191 (2000) 30.
- [21] P.V. Alston, D.D. Shillady, J. Org. Chem. 39 (1974) 3402.
- [22] A.B. Sherrill, H. Idriss, M.A. Barreau, J.G. Chen, Catal. Today 85 (2003) 321.
- [23] L. Benz, J. Haubrich, R.G. Quiller, C.M. Friend, Surf. Sci. 603 (2009) 1010.
- [24] C.J. Kiewer, M. Bieri, G.A. Somorjai, J. Am. Chem. Soc. 131 (2009) 9958.
- [25] J.C.D. Jesús, F. Zaera, Surf. Sci. 430 (1999) 99.
- [26] J.Q. Fu, C.H. Ding, Catal. Commun. 6 (2005) 770.
- [27] L.E. Murillo, J.G. Chen, Surf. Sci. 602 (2008) 919.
- [28] S. Pirillo, I. López-Corral, E. Germán, A. Juan, Appl. Surf. Sci. 263 (2012) 79.
- [29] M. Akita, N. Osaka, K. Itoh, Surf. Sci. 405 (1998) 172.
- [30] S. Thakur, V.P. Gupta, B. Ram, Spectrochim. Acta A 53 (1997) 749.
- [31] S. Fujii, N. Osaka, M. Akita, K. Itoh, J. Phys. Chem. 99 (1995) 6994.
- [32] F. Delbecq, P. Sautet, J. Catal. 152 (1995) 217.
- [33] F. Delbecq, P. Sautet, J. Catal. 211 (2002) 398.
- [34] S. Iizumi, S. Ninomiya, M. Sekine, M. Nakata, J. Mol. Struct. 1025 (2012) 43.
- [35] S. Damyanova, M.A. Centeno, L. Petrov, P. Grange, Spectrochim. Acta A 57 (2001) 2495.
- [36] G.B. Chernobay, Y.A. Chesarov, V.P. Baltakhinow, G.Y. Popova, T.V. Andrushkevich, Catal. Today 164 (2011) 58.
- [37] R.W. Stevens Jr., S.C. Chuang, B.H. Davis, Appl. Catal. A 252 (2003) 57.
- [38] J.K. Jiang, Z.L. Zhang, J.Y. Li, T.D. Li, Leather Chem. (China) 25 (2008) 5.